Eur. Phys. J. D **9**, 377–380 (1999)

THE EUROPEAN PHYSICAL JOURNAL D

EDP Sciences

Degeneracy and repulsion between bands of periodic carbon nanotube junctions

R. Tamura and M. Tsukada

Department of Physics, Graduate School of Science, University of Tokyo, Hongo 7-3-1, Bunkyo-ku, Tokyo 113, Japan

Received: 26 August 1998

Abstract. The band structures of the periodic nanotube junctions are investigated by the use of effective mass theory ($k \cdot p$ approximation) and the tight binding model. The periodic junctions are constructed by the periodic introduction of defect pairs, consisting of a pentagonal defect and a heptagonal defect, into the carbon nanotube. We treat the periodic junctions whose unit cell is composed by two kinds of metallic nanotubes. The discussed energy region is near the undoped Fermi level where the channel number is kept to 2, so there are two bands. The degeneracy and repulsion between the two bands are determined only from symmetries.

PACS. 72.80.Rj Fullerenes and related materials – 73.20.Dx Electron states in low dimensional structures (superlattices, quantum well structures and multilayers) – 72.10.Fk Scattering by point defects, dislocations, surfaces, and other imperfections (including Kondo effect)

A carbon nanotube is a one-dimensional structure formed when the honeycomb lattice of the monolayer graphite is rolled up [1]. Its radius and length are measured in nanometers and micrometers, respectively. One of the carbon nanotube's interesting features, theoretically predicted [2] and investigated experimentally [3], is that it becomes metallic or semiconducting according to the radius and the helicity of the honeycomb lattice forming the tube. Metallic nanotubes especially are expected to be used as electric leads with nanometer size. Thus we concentrate our discussion in this paper on metallic nanotubes.

A junction connecting different nanotubes can be formed without dangling bonds by the introduction of a defect pair, consisting of a pentagonal defect and a heptagonal defect [4–8]. Such defects are called disclinations and are necessary for the formation of various structures composed of curved surface of graphitic layer [9, 10]. Among them, we treat the periodical multiple nanotube junctions in this paper, some of which have helical forms [11, 12]. We have already obtained an analytical expression of the transmission rate of the single junction. It is irrespective of the angle between the two tube axes, and determined only by the ratio of the circumferences of the nanotubes and the ratio $|E/E_c|$, where E_c is the threshold energy above which the channel number increases [13]. In this paper, we will show that some qualitative features of the band structures of the periodical junctions can be derived only by their symmetries.

The bond network of the nanotube junction is represented by the development map, Fig. 1. The circumference of the tube in the development map is denoted by the vector $\mathbf{R_j}$ $(j = 5, 7)$. Here we use two pairs of the vectors $\{\mathbf{e}_1, \mathbf{e}_2\}$ and $\{\mathbf{e}_x, \mathbf{e}_y\}$, where $\mathbf{e}_x = (\mathbf{e}_1 + \mathbf{e}_2)/\sqrt{3}$, and $\mathbf{e}_y = \mathbf{e}_2 - \mathbf{e}_1$ represent vectors on the development map. $\mathbf{e}_1$ and

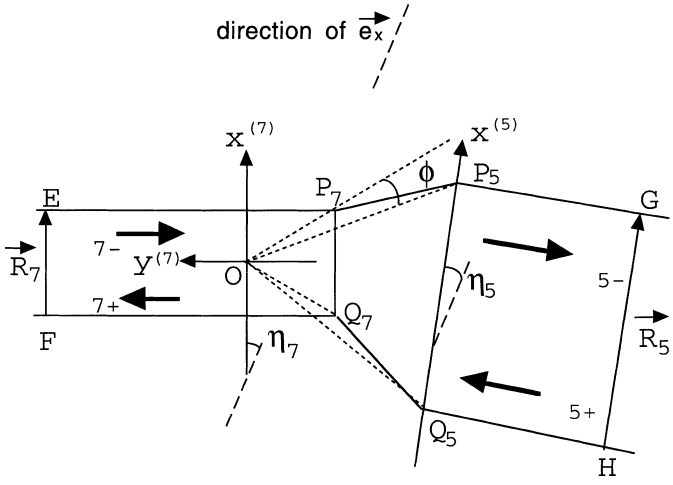

Fig. 1. Development map of the nanotube junctions. The lines EP_7, P_7P_5, P_5G are connected and become identical with the lines FQ_7, Q_7Q_5, and Q_5H, respectively. The rectangles EP_7Q_7F and P_5GHQ_5 form the thinner tube and the thicker tube, respectively. P_7P_5 is Q_7Q_5 rotated by an angle of 60 degrees, and the quadrilateral $P_7P_5Q_5Q_7$ forms a junction with the shape of a part of a cone. A heptagonal defect and a pentagonal defect are introduced at $P_7(=Q_7)$ and $P_5(=Q_5)$, respectively. The equilateral triangles ΔOP_7Q_7 and ΔOP_5Q_5, with bases P_7Q_7 and P_5Q_5, have common apex O, which is taken to be the origin of the polar coordinate (r, θ).

$\mathbf{e}_2$ are the basic translation vectors of 2D graphite, and the angle between them is $\pi/3$, while that between $\mathbf{e}_x$ and $\mathbf{e}_y$ is $\pi/2$. The four vectors have a common length of about 0.25 nm, denoted by a hereafter. In this paper, we concentrate our discussion on the metallic nanotube, so that only the tube of which $R_1 - R_2$ is an integer multiple of three is considered [2]. The positions of the sublattices A and B are represented by $\mathbf{q} = (q_1, q_2)$ and at $\mathbf{q}+\boldsymbol{\tau} = (q_1 + \frac{1}{3}, q_2 + \frac{1}{3})$, respectively, with integer components q_1 and q_2. In the effective mass theory ($k \cdot p$ approximation), their wavefunction amplitude, $\psi_A(\mathbf{q})$ and $\psi_B(\mathbf{q})$, is represented by

$$\psi_i(\mathbf{q}) = F_i^K(\mathbf{q}) w^{(q_1-q_2)} + F_i^{K'}(\mathbf{q}) w^{(q_2-q_1)} \quad (i = A, B), \tag{1}$$

where $w \equiv \exp(i2\pi/3)$ and $F_{A,B}^{K,K'}$, $w^{(q_1-q_2)}$, $w^{(q_2-q_1)}$ are the envelop wave functions and the Bloch state wave function at the K point and that at the K' point, respectively.

A tight binding model with only a π orbital is used, where nearest-neighbor hopping integrals and site energies are taken to be γ and zero, which are common for any sites. By substituting (1) in the tight binding model, one obtains [14]

$$\frac{\sqrt{3}}{2}\gamma a\,(-i\partial_y + \partial_x) F_B^K = E F_A^K, \tag{2}$$

$$\frac{\sqrt{3}}{2}\gamma a\,(-i\partial_y - \partial_x) F_A^K = E F_B^K \ . \tag{3}$$

Here, only the first-order term in the Taylor expansion of the envelop functions, F, is taken. When E is close to zero, it is a good approximation, because spatial variance of the envelop function is slow compared to the lattice constant, a. The equations of the envelop wave functions $F_{A,B}^{K'}$ can be easily obtained by $-i \to i$ in (2) and (3). Hereafter the envelop wave functions F are often simply called the wave functions. When plane wave functions $\exp(i\mathbf{k}\cdot\mathbf{q})$ are applied to F in (2) and (3), one gets an isotropic linear dispersion relation,

$$E = \frac{\sqrt{3}}{2}\gamma a|\mathbf{k}|. \tag{4}$$

The boundary condition is $\mathbf{k}\cdot\mathbf{R} = 2\pi l$, with an integer l. Discussions in this paper concentrate on the case when E is so close to zero that only $l = 0$ is permitted, i.e., $\mathbf{k}$ is parallel to the tube axis. Therefore

$$F_A(\mathbf{q})/F_B(\mathbf{q}) = \pm\exp(-i\eta) \ , \tag{5}$$

where η is the angle of $\mathbf{R}$ with respect to the x axis.

The amplitude of the plane wave in each tube part, which is denoted by α, is obtained from (5) as

$$\alpha_{j\pm}^K = \frac{1}{\sqrt{2R_j}} \int_{Q_j}^{P_j} \mathrm{d}x^{(j)} \left(e^{i\frac{\eta_j}{2}} F_A^K \pm e^{-i\frac{\eta_j}{2}} F_B^K \right) \quad (j = 5, 7) \tag{6}$$

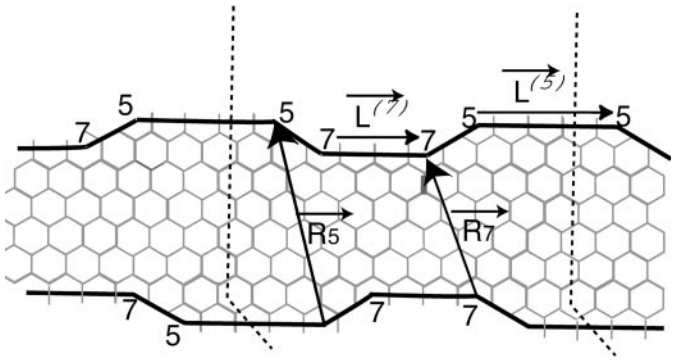

Fig. 2. Development map of the periodic junctions. The positions of the pentagonal defects and heptagonal defects are denoted by the numbers 5 and 7, respectively. The upper bold line is connected with the lower bold lines, so that the points connected by the circumference vectors become identical. In this figure, $\mathbf{R_5} = (2, 5)$, $\mathbf{R_7} = (1, 4)$, $\mathbf{L^{(5)}} = (4, -4)$, and $\mathbf{L^{(7)}} = (3, -3)$. The area between the two dotted lines is the unit cell of the periodic junctions.

for the K point. The indices $+$ and $-$ mean directions in which the electronic waves propagate. Equations for $\alpha_{j\pm}^{K'}$ are obtained from (6) by the replacement of $\pm$ and K in the r.h.s with $\mp$ and K', respectively.

Figure 2 shows the unit cell of the periodic junctions, which is determined by four vectors: the circumference of the thicker tube $\mathbf{R_5}$, that of the thinner tube $\mathbf{R_7}$, and the vector connecting the two pentagons (heptagons) in the thicker and thinner tube parts, $\mathbf{L^{(5)}}$ and $\mathbf{L^{(7)}}$, respectively. Transfer of the plane wave from the thicker tube to the thinner tube is represented by a transfer matrix:

$$\begin{pmatrix} \boldsymbol{\alpha}_{7+} \\ \boldsymbol{\alpha}_{7-} \end{pmatrix} = \begin{pmatrix} t_1, t_2^* \\ t_2, t_1^* \end{pmatrix} \begin{pmatrix} \boldsymbol{\alpha}_{5+} \\ \boldsymbol{\alpha}_{5-} \end{pmatrix} \ . \tag{7}$$

By combining the transfer matrices, the two energy bands of the periodic junctions, $k_+^{(p)}$ and $k_-^{(p)}$, are obtained from t_1 and t_2 as

$$\cos\left(k_\pm^{(p)}\right) = \frac{1}{2}\left(X_{11} + X_{22} \pm \sqrt{(X_{11} - X_{22})^2 + 4X_{21}^2 - 4Y_{21}^2} \right), \tag{8}$$

where

$$X \equiv \mathrm{Re}\left\{ \Lambda_5^{1/2} ({}^t t_1 \Lambda_7 t_1 - {}^t t_2 \Lambda_7^{-1} t_2) \Lambda_5^{1/2} \right\} \ ,$$
$$Y \equiv \mathrm{Re}\left\{ \Lambda_5^{-1/2} (t_1^\dagger \Lambda_7^{-1} t_2 - t_2^\dagger \Lambda_7 t_1) \Lambda_5^{1/2} \right\} \ . \tag{9}$$

Here, Λ represents the phase factor of the plane wave in the tube part:

$$\Lambda_j = \exp(i\mathbf{k_j}\cdot\mathbf{L^{(j)}}) \begin{pmatrix} w^{l_j}, & 0 \\ 0, & -w^{-l_j} \end{pmatrix}, \tag{10}$$

where $l_j \equiv L_1^{(j)} - L_2^{(j)}$ and $j = 5, 7$. Since $w^3 = 1$, l_j can take a value of either 0 or $\pm 1 \pmod 3$. The factor $\exp(i\mathbf{k_j}\cdot\mathbf{L^{(j)}})$

comes from the envelop functions F, and the other part comes from the Bloch states at K or K'.

To discuss the symmetry, we use the scattering matrix S. The scattering matrix S determines the outgoing waves for the incoming waves as

$$\begin{pmatrix} \boldsymbol{\alpha_{5-}} \\ \boldsymbol{\alpha_{7+}} \end{pmatrix} = \begin{pmatrix} r_5, t \\ {}^t t, r_7 \end{pmatrix} \begin{pmatrix} \boldsymbol{\alpha_{5+}} \\ \boldsymbol{\alpha_{7-}} \end{pmatrix} \ , \tag{11}$$

where $\boldsymbol{\alpha}_+ = {}^t(\alpha_+^K, \alpha_+^{K'})$ and $\boldsymbol{\alpha}_- = {}^t(\alpha_+^{K'}, \alpha_+^K)$, each component of which is defined in (6). The relation between (7) and (11) is represented as

$$t_1 = (1/t)^*, \quad t_2 = -(1/t) r_5 \ . \tag{12}$$

Consider the operation Q_1 defined as $Q_1(F_A^K, F_B^K, F_A^{K'}, F_B^{K'}) = (-F_B^{K'}, F_A^{K'}, F_B^K, -F_A^K)$. The amplitude $\boldsymbol{\alpha}$ is transformed by this operation Q_1 as

$$Q_1 \boldsymbol{\alpha}_\pm = \pm \begin{pmatrix} 0,1 \\ 1,0 \end{pmatrix} \boldsymbol{\alpha}_\pm \equiv \pm \sigma_1 \boldsymbol{\alpha}_\pm \ . \tag{13}$$

Since the effective mass theory equations (2) and (3) and the boundary conditions are invariant under the operation Q_1,

$$-\sigma_1 r_j \sigma_1 = r_j, \quad \sigma_1 t \sigma_1 = t \quad (j = 5, 7). \tag{14}$$

It is generally guaranteed by conservation of flow and time reversal symmetry that S is a symmetric unitary matrix. This general condition and the condition (14) determine the form of S as

$$r_j = \sqrt{R} e^{ip_j} \begin{pmatrix} 1, & 0 \\ 0, & -1 \end{pmatrix} \quad (j = 5, 7), \tag{15}$$

and

$$t = \sqrt{T} e^{i(p_5 + p_7)} \begin{pmatrix} \cos(f), i\sin(f) \\ i\sin(f), \cos(f) \end{pmatrix} \ , \tag{16}$$

where R and $T = 1 - R$ are the reflection rate and the transmission rate, respectively, while p_j and f are certain real values. The meaning of f is discussed below.

Consider operation Q_2 shown in Fig. 3. Under the operation Q_2, the upper development map is transformed into the lower development map and the angle between the two tube axes in the development map, $\phi \equiv \eta_7 - \eta_5$, decreases by $\pi/3$ as $\phi' = \phi - \pi/3$. The two development maps in Fig. 3 correspond to identical junctions. The only difference is how the cutting line on the honeycomb plane of the junction is drawn. Therefore the S matrix of the upper development map becomes the same as that of the lower one, after a unitary transformation corresponding to the operation Q_2. The boundary condition in the junction part is

$$\left(F_A^K, F_B^K, F_A^{K'}, F_B^{K'}\right)|_{\theta+\pi/3} = \left(\frac{1}{w} F_B^{K'}, w F_A^{K'}, w F_B^K, \frac{1}{w} F_A^K\right)|_\theta \ , \tag{17}$$

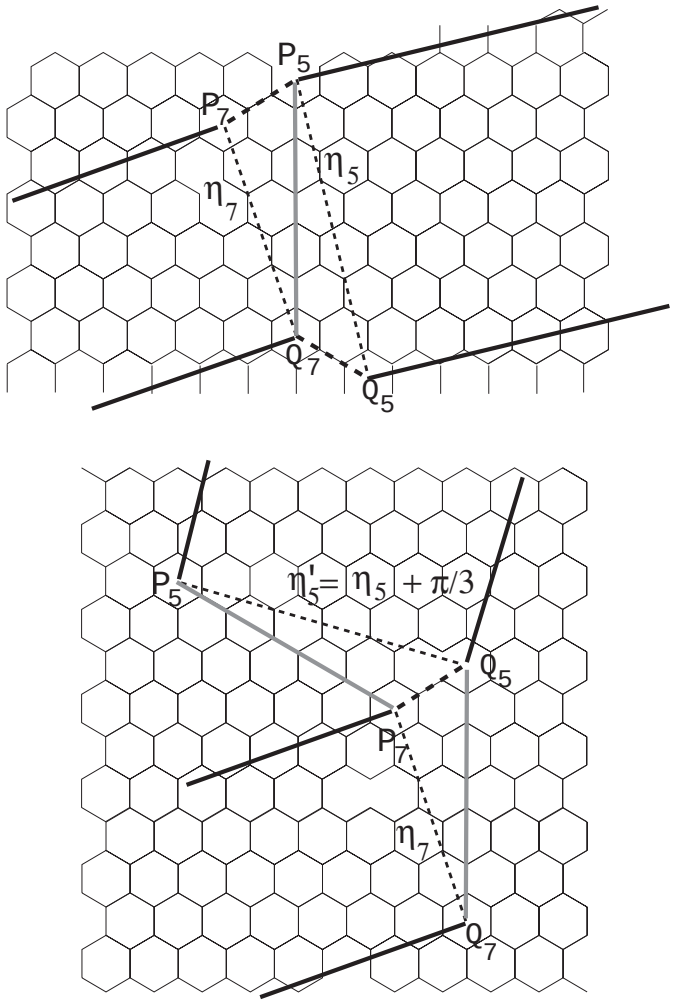

Fig. 3. The operation Q_2, which fixes the thinner tube part but rotates the thicker tube part by $\pi/3$ in the development map. The upper development map is transformed into the lower one under the operation Q_2. These two development maps correspond to the identical junctions, denoted by the (1,4)–(2,5) junctions.

where the polar coordinate defined in Fig. 1 is used [13, 15]. By using it and $\eta_5' = \eta_5 + \pi/3$ in (6), we get

$$Q_2 \boldsymbol{\alpha_{5\pm}} = \pm i \sigma_1 \boldsymbol{\alpha_{5\pm}}, \tag{18}$$

while $Q_2 \boldsymbol{\alpha}_{7\pm} = \boldsymbol{\alpha}_{7\pm}$. From this symmetry, we can derive

$$\begin{aligned} r_5(\phi - \pi/3) &= -\sigma_1 r_5(\phi) \sigma_1 \\ t(\phi - \pi/3) &= -i \sigma_1 t(\phi) \ , \end{aligned} \tag{19}$$

which leads to

$$f(\phi) = f(0) + \frac{3}{2}\phi \ . \tag{20}$$

Finally, we consider the coordinate transformation from the right-handed coordinate to the left-handed coordinate Q_3, $(x, y) \to (-x, y)$. It causes $\eta_j \to -\eta_j$, $\phi \to -\phi$, and exchange between the sublattices, $Q_3(F_A^K, F_B^K, F_A^{K'}, F_B^{K'}) =$

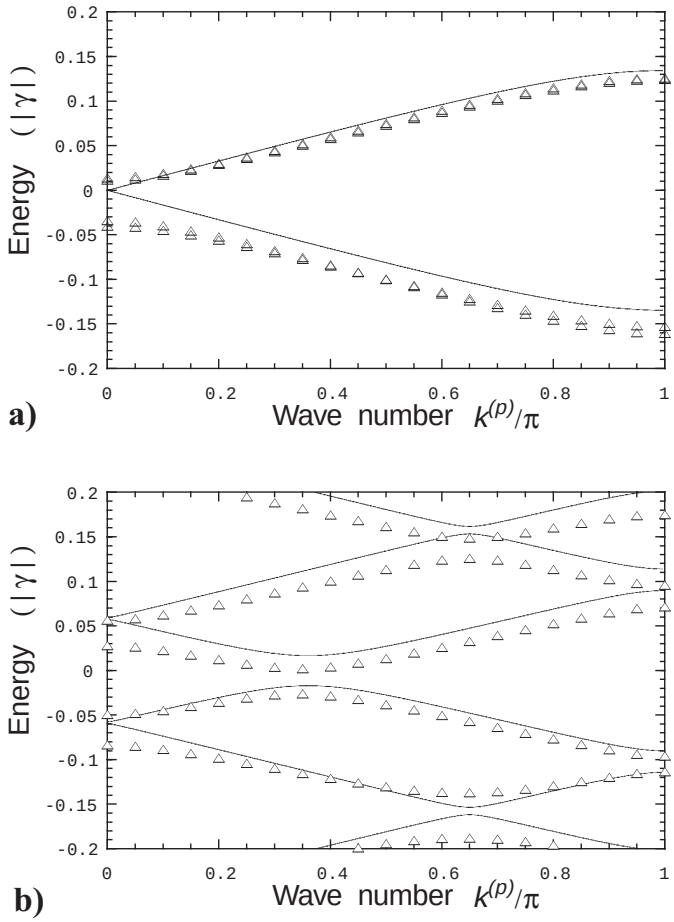

Fig. 4. The band structures of the periodic junctions. The vertical axis is the energy in units of the absolute value of the hopping integral, $|\gamma| = -\gamma$. Triangles and solid lines are the results from the tight binding model and those from the effective mass equations, respectively. These coincide fairly well. (a) $l_5 = l_7 = 0$ and $\phi \simeq 0.034\pi$. $\mathbf{R_7} = (1, 10)$, $\mathbf{R_5} = (3, 12)$, $\mathbf{L^{(7)}} = (4, -5)$, and $\mathbf{L^{(5)}} = (6, -3)$. (b) $l_5 l_7 = -1$ and $\phi \simeq 0.14\pi$. $\mathbf{R_7} = (10, 1)$, $\mathbf{R_5} = (7, 7)$, $\mathbf{L^{(7)}} = (6, -5)$, and $\mathbf{L^{(5)}} = (13, -6)$.

$(F_B^K, F_A^K, F_B^{K'}, F_A^{K'})$, so that

$$Q_3 \boldsymbol{\alpha}_\pm = \begin{pmatrix} 1, & 0 \\ 0, & -1 \end{pmatrix} \boldsymbol{\alpha}_\pm \equiv \sigma_2 \boldsymbol{\alpha}_\pm \ . \tag{21}$$

The result is

$$\begin{aligned} r_j(-\phi) &= \sigma_2 r_j(\phi) \sigma_2 \quad (j = 5, 7) \\ t(-\phi) &= \sigma_2 t(\phi) \sigma_2 \ , \end{aligned} \tag{22}$$

which indicates that

$$f(0) = 0 \tag{23}$$

in (20).

As for the factors T and p_j, one has to solve the effective mass equations to get more information on them, but there is an important result obtained solely from the argument of the symmetries. As is shown in Fig. 4a, the two bands $k_+^{(p)}$ and $k_-^{(p)}$ are almost degenerate when $l_5 = l_7 = 0$. On the other hand, the two bands avoid each other when $l_5 l_7 = 1$, $\phi \neq 0$, or $l_5 l_7 = -1$, $\phi \neq \pi/3$ as is shown in Fig. 4b. These can be explained from (8). The origin of the degeneracy in the former case is that both X and Y are diagonal and $X_{11} = X_{22}$ [16]. The origin of the repulsion between the bands in the latter case is that Y has nonzero off-diagonal elements. These origins can be derived only from (15), (16), (20), and (23), without solution of the effective mass equations.

We wish to thank Dr. K. Akagi for showing us his numerical data. We would like to thank Mr. H. Matsumura and Professor T. Ando for their useful suggestions. This work has been supported by the Core Research for Evolutional Science and Technology (CREST), of the Japan Science and Technology Corporation (JST).

References

1. S. Iijima: Nature (London) **354**, 56 (1991)
2. R. Saito *et al.*: Phys. Rev. B **46**, 1804 (1992); J.W. Mintmire *et al.*: Phys. Rev. Lett. **68**, 631 (1992); N. Hamada *et al.*: Phys. Rev. Lett. **68**, 1579 (1992)
3. M. Bockrath *et al.*: Science **275**, 1922 (1997); T.W. Ebbesen *et al.*: Nature **382**, 54 (1996); A.Yu. Kasumov *et al.*: Europhys. Lett. **34**, 429 (1996); L. Langer *et al.*: Phys. Rev. Lett. **76**, 479 (1996); S.J. Tans *et al.*: Nature (London) **386**, 474 (1997); S. Frank *et al.*: Science **280**, 1774 (1998)
4. S. Iijima, T. Ichihashi, Y. Ando: Nature (London) **356**, 776 (1992)
5. R. Tamura, M. Tsukada: Phys. Rev. B **55**, 4991 (1997)
6. R. Tamura, M. Tsukada: Z. Phys. D **40**, 432 (1997)
7. R. Saito, G. Dresselhaus, M.S. Dresselhaus: Phys. Rev. B **53**, 2044 (1996)
8. L. Chico *et al.*: Phys. Rev. Lett. **76**, 971 (1996); L. Chico *et al.*: Phys. Rev. B **54**, 2600 (1996); T. Nakanishi, T. Ando: J. Phys. Soc. Jpn. **66**, 2973 (1997); J.-C. Charlier, T.W. Ebbesen, Ph. Lambin: Phys. Rev. B **53**, 11 108 (1996); M. Menon, D. Srivastava: Phys. Rev. Lett. **79**, 4453 (1997); V. Meunier, L. Henrard, Ph. Lambin: Phys. Rev. B **57**, 2586 (1998)
9. R. Tamura, M. Tsukada: Phys. Rev. B **49**, 7697 (1994)
10. R. Tamura *et al.*: Phys. Rev. B **56**, 1404 (1997); S. Ihara *et al.*: Phys. Rev. B **54**, 14 713 (1996)
11. K. Akagi *et al.*: Phys. Rev. B **53**, 2114 (1996); K. Akagi *et al.*: Phys. Rev. Lett. **74**, 2307 (1995)
12. S. Amelinckx *et al.*: Science **265**, 635 (1994); X.B. Zhang *et al.*: Europhys. Lett. **27**, 141 (1994); S. Ihara, S. Itoh, J. Kitakami: Phys. Rev. B **48**, 5643 (1993)
13. R. Tamura, M. Tsukada: Phys. Rev. B **58**, 8120 (1998); R. Tamura, M. Tsukada: J. Phys. Soc. Jpn. **68**, 910 (1999)
14. H. Ajiki, T. Ando: J. Phys. Soc. Jpn. **65**, 2976 (1996); T. Ando, T. Nakanishi: J. Phys. Soc. Jpn. **67**, 1704 (1998)
15. H. Matsumura, T. Ando: J. Phys. Soc. Jpn. **67**, 3542 (1998)
16. The bands calculated by the tight binding model are almost degenerate, but slightly split due to higher-order terms of $k \cdot p$ in the effective mass equations, which make the equations variant under the operation Q_1. The invariance under the operation Q_1 holds within the linear approximation with $k \cdot p$.